Integration, Validation, and Application of a PV Snow Coverage Model in SAM

David Ryberg and Janine Freeman
National Renewable Energy Laboratory

NREL is a national laboratory of the U.S. Department of Energy
Office of Energy Efficiency & Renewable Energy
Operated by the Alliance for Sustainable Energy, LLC

This report is available at no cost from the National Renewable Energy Laboratory (NREL) at www.nrel.gov/publications.

Technical Report
NREL/TP-6A20-64260
September 2015

Contract No. DE-AC36-08GO28308

NREL
NATIONAL RENEWABLE ENERGY LABORATORY

Integration, Validation, and Application of a PV Snow Coverage Model in SAM

David Ryberg and Janine Freeman
National Renewable Energy Laboratory

Prepared under Task No. SS13.5020

NREL is a national laboratory of the U.S. Department of Energy
Office of Energy Efficiency & Renewable Energy
Operated by the Alliance for Sustainable Energy, LLC

This report is available at no cost from the National Renewable Energy Laboratory (NREL) at www.nrel.gov/publications.

National Renewable Energy Laboratory
15013 Denver West Parkway
Golden, CO 80401
303-275-3000 • www.nrel.gov

Technical Report
NREL/TP-6A20-64260
September 2015

Contract No. DE-AC36-08GO28308

NOTICE

This report is available at no cost from the National Renewable Energy Laboratory (NREL) at www.nrel.gov/publications.

Available electronically at SciTech Connect http:/www.osti.gov/scitech

Available for a processing fee to U.S. Department of Energy and its contractors, in paper, from:

U.S. Department of Energy
Office of Scientific and Technical Information
P.O. Box 62
Oak Ridge, TN 37831-0062
OSTI http://www.osti.gov
Phone: 865.576.8401
Fax: 865.576.5728
Email: reports@osti.gov

Available for sale to the public, in paper, from:

U.S. Department of Commerce
National Technical Information Service
5301 Shawnee Road
Alexandria, VA 22312
NTIS http://www.ntis.gov
Phone: 800.553.6847 or 703.605.6000
Fax: 703.605.6900
Email: orders@ntis.gov

Cover Photos by Dennis Schroeder: (left to right) NREL 26173, NREL 18302, NREL 19758, NREL 29642, NREL 19795.

NREL prints on paper that contains recycled content.

Abstract

Due to the increasing deployment of photovoltaic (PV) systems in snowy climates, there is significant interest in a method capable of estimating PV losses resulting from snow coverage that has been verified for a variety of system designs and locations. Many independent snow coverage models have been developed over the last 15 years; however, there has been little effort verifying these models beyond the system designs and locations on which they were based. Moreover, major PV modeling software products have not yet incorporated any of these models into their workflows. In response to this deficiency, we have integrated the methodology of the snow model developed in the paper by Marion et al. (2013) into the National Renewable Energy Laboratory's (NREL) System Advisor Model (SAM). In this work, we describe how the snow model is implemented in SAM, and we discuss our demonstration of the model's effectiveness at reducing error in annual estimations for three PV arrays. Next, we use this new functionality in conjunction with a long-term historical data set to estimate average snow losses across the United States for two typical PV system designs. The open availability of the snow loss estimation capability in SAM to the PV modeling community, coupled with our results of the nationwide study, will better equip the industry to accurately estimate PV energy production in areas affected by snowfall.

Introduction

Snow coverage of PV systems and the associated losses in energy production have been recognized by the PV community as a significant loss that must be accounted for (Marion et al. 2013; Becker et al. 2006; Powers, Newmiller, and Townsend 2010; Andrews, Pollard, and Pearce 2013; Sugiura et al. 2003). However, the convoluted dynamics of snow coverage on PV systems (snow removal processes in particular), in addition to the large variability in determining a location's typical snowfall over the course of a year, have made a reliable model capable of estimating these losses infeasible for general use. Previous studies on this topic have measured losses in annual energy production ranging from 0% (Andrews, Pollard, and Pearce 2013) to 25% (Powers, Newmiller, and Townsend 2010). Of course, these studies vary substantially in terms of the type of the PV array employed and the physical location in which the study took place. Moreover, several empirical models have been developed by the community that can estimate these losses (Townsend and Powers 2011; Andrews and Pearce 2012); however, in almost all cases there has been little or no effort to verify these models beyond the systems on which their design was based. There is a clear need within the community for a model capable of reliably predicting PV snow losses for a variety of PV system types and in a variety of locations.

For this purpose, we have integrated the PV snow coverage model developed by Marion et al. (2013) into the National Renewable Energy Lab's (NREL) System Advisor Model (SAM). The following report details the methodology of the model's implementation, the results of a validation study against three PV systems that were not involved in the model's creation, and finally, the results of a national study using the new snow model in SAM.

Implementation

Marion's Model

The PV snow coverage model in Marion et al. (2013) calculates the percentage of a PV array that will be covered by snow given system tilt, daily snow depth measurements, and hourly plane of array (POA) irradiance and temperature values. The model considers snow sliding to be the dominant removal process and therefore does not account for snow melting or wind removal (except in the case of flat fixed-tilt systems). Other works, independent of Marion's analysis, have also expressed snow sliding as a dominant removal process (Becker et al. 2006; Andrews, Pollard, and Pearce 2013; Sugiura et al. 2003). A brief description of Marion's model is as follows.

At the beginning of each day, the model checks to see if a snowfall has occurred during that day. If it has, the model assumes that the PV array being simulated will be completely covered by snow. If a new snowfall is not detected, the coverage is left at its value at the end of the previous day. For each hour in the day, the array will remain covered unless the plane of array irradiance and ambient temperature are sufficient to allow some of the accumulated snow to slide off the PV array. More specifically, snow sliding will only occur so long as the following inequality is satisfied:

$$T_a > \frac{I_{poa}}{m}$$

where T_a represents the ambient temperature, I_{poa} represents the plane of array irradiance, and m represents Marion's empirically defined value $-80\ W/(m\text{^}2\ ^\circ C)$. If the model determines that sliding is possible during a particular hour, then the amount of the PV array that will be exposed in that hour, measured in tenths of a row's total height (see Figure 1), is a function of the PV system's tilt.

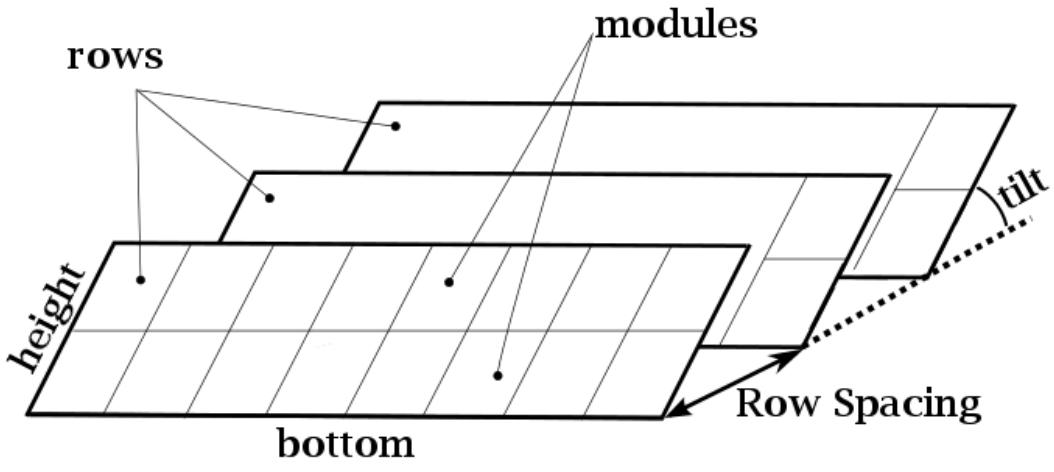

Figure 1. Simplified diagram of a PV array

The amount that will be exposed, in tenths of total row height, can be found using:

$$Snow\ Slide\ Amount = 1.97 * \sin(\ tilt\ )$$

The 1.97 constant in this equation was experimentally determined by Marion et al. (2013) for roof-mounted systems in units of tenths of PV row height per hour, and will be referred to as the *sliding coefficient*. At the end of the hour during which the calculation permits sliding, the initial PV snow coverage will be decremented by the snow slide amount. Finally, given the new height of snow relative to the PV row's total height, and the configuration of PV strings in a row, the number of PV strings within the system which are not covered with snow is determined. These modules are allowed to operate normally while the energy production of the covered strings is set to zero. The model then moves on to the next hour in the day and repeats this process.

Marion et al. (2013) also provided a sliding coefficient for ground-mounted systems, which is reported as 6.0 tenths of PV row height per hour. The discrepancy between this value and the 1.97 value stems from the necessity of roof mounted systems to account for snow accumulating at the lower edge of an array and preventing snow removal from the lower modules. To date, however, only the sliding coefficient for roof-mounted systems has been incorporated into SAM because it was determined from a larger sample size in Marion's analysis and is therefore better validated.

Implementation in SAM

The final implementation of Marion et al.'s (2013) model in SAM is procedurally very similar to Marion's original model; however, there are a small number of differences that warrant discussion. Two of the changes were overrides that prevent illogical behavior. The first of these simply checks the snow coverage at the end of each time step and prevents the coverage from going below 0%. Second, when calculating the snow coverage at the beginning of each time step, we included an additional check for zero snow depth at that time. We assume that if the snow depth at that time is zero, then the coverage percentage on the PV array should also be zero. Without this check, snow would never slide off of zero-degree fixed-tilt PV arrays once it had accumulated. This second check was not required in Marion's original model since that model was designed for system tilts between 10° and 45°. However, as we will discuss in the validation section, with this override the implemented PV snow coverage model also proves reasonable for flat systems.

Following this, by conducting a review of the currently available snow depth sensors, we found that many devices have an uncertainty between 0.5 and 1.0 cm. Therefore, we also included threshold values for minimum depth and minimum change in depth (delta), which are intended to filter out noise in the snow depth measurements and reduce spurious responses to data measurement uncertainty, such as findings of new snowfall during summer months. We incorporated these thresholds within the portion of the implementation that determines whether a new snowfall has occurred. If the original model identifies a new snowfall but either the total snow depth is less than the depth threshold or the change in snow depth (with respect to the previous time step's depth) is less than the delta threshold, then we assume this is an erroneous detection and it is ignored. We set the depth threshold to 1 cm and the delta threshold to 1 cm/hour for consistency with snow depth measurement uncertainties; an additional sensitivity

analysis on these threshold values indicated that varying the threshold values within a range of 0.5 to 1.5 cm and cm/hour respectively do not significantly affect estimated snow losses.

Lastly, Marion's original model applied snow losses for an hourly simulation using a daily snow depth data set which was measured every day at 7am. However, SAM users may have access to more granular snow depth data. Additionally, SAM is capable of simulating PV performance for sub-hourly time intervals. Therefore, it was necessary to adapt the snow model's implementation to allow for the usage of hourly and sub-hourly snow depth data sets as well as to accommodate sub-hourly simulations.

First, we sought to determine if the model would lose accuracy if the check for a new snowfall is performed hourly versus once a day. In order to compare the two methods fairly, we fabricated an hourly snow depth data set from a pre-existing daily data set by setting each hour in a single day to the snow depth record of the corresponding day in the daily set. Then, we executed the model in both its original daily form (including the changes discussed up until this point) and in another form that checks for a new snowfall at the start of each hour. We found that, as expected, the two methods produced identical results. Similarly, we conducted another study where we considered NREL's Research Support Facility 2 (RSF2) PV array, which has hourly measured power outputs and meteorological data, including hourly snow depth data. We converted the hourly snow depth data for this site to a daily data set (by setting all values in a day to the value at 7 a.m. in the hourly set in accordance with Marion's data collection procedure) and ran simulations in SAM with both sets. We found that the simulation with the hourly data set resulted in noticeably less error in annual energy compared to measured data than the simulation with the daily data (from a 2.3% error using the daily data to a 0.1% error for the hourly data). The method used to calculate these errors will be discussed further in the validation section. Because checking for a new snowfall at the beginning of hour as opposed to at the beginning of each day produced no difference when a daily snow depth data set was converted to an hourly set, and because the algorithm was shown to lose accuracy when the opposite conversion was performed, we decided to check for a new snowfall at the beginning of each time step for the final implementation.

Second, we accounted for sub-hourly calculations. The workflow of the snow model is unchanged with the exception that the sliding coefficient and the delta threshold, which were originally determined as hourly values, are both scaled by the inverse of the number of time steps in an hour. For example, if SAM is provided with 15-minute weather data, then the sliding coefficient and the delta threshold are each multiplied by 0.25 to convert them from hourly to 15-minute values.

Snow Model Usage in SAM

The resulting PV snow coverage model can be accessed in two separate ways: by running the model in conjunction with an ongoing PV simulation or by invoking the model after a complete PV simulation has occurred. In the desktop version of SAM, the snow model can be activated by navigating to the 'Shading and Snow' design page and selecting the 'Estimate losses due to snow' check box. Doing so will instruct the snow model to run in conjunction with the PV simulation and will logically be applied at the same point as similar losses (shading and soiling). In SAM's workflow, this occurs after losses associated with the modules themselves (module efficiency and degradation) are applied, but before the inverter model is run. The same behavior

can be achieved either through SAM's LK scripting language or in one of the SDK extension languages by setting the 'en_snow_model' variable to 1; its default value is 0, which deactivates the snow model. Once the snow model is activated, a SAM PV simulation can be executed normally and the final power reports will reflect snow loss estimations. Moreover, time series arrays of the amount of energy lost in each subarray due to snow coverage can be accessed through the 'subarray[*n*]_snow_loss' variables, where [*n*] is replaced with a specific subarray's identification number. For more information on how to use SAM's LK scripting language or access the SDK, visit the SAM webpage at sam.nrel.gov.

The second method of accessing the snow model—invoking the model after a simulation has occurred—can only be accomplished by using either SAM's LK scripting language or through the SDK. Additionally, invoking the snow model in this manner requires that a time series array of the modeled system's energy output be provided as an input to the snow model. This can be accomplished in one of two ways: 1) by executing a full SAM PV simulation, without having activated the snow model, in which case the required output variable will already be present in the SAM instance, or 2) by manually providing an energy output array, through the method discussed in SAM's operating manual, and defining it as the 'gen' variable. The input 'gen' array can be either DC or AC energy, a fact which we will discuss next. Once invoked, the snow model will calculate loss estimates due to snow coverage at each time step and will deduct the appropriate losses from the initial energy time series. Regardless of when the snow model is applied, its success is dependent on the input weather file containing valid snow depth data.

AC Versus DC Side Application

Snow coverage on PV arrays immediately results in a decreased DC power output by the array, so it makes the most sense to apply the losses estimated by a snow model at the same time that similar losses (shading and soiling) are applied. The empirical correlations in Marion's model, however, were formulated using the measured AC power, so we examined whether the model is still valid when applied to the DC side of power conversion.

As discussed previously, the way in which the model was implemented into SAM allows for execution of the snow model either simultaneously with SAM's PV model workflow—equivalent to applying snow losses on the DC side of power conversion—or independently after a SAM PV simulation has completed—equivalent to AC-side application. Fortunately, this made comparing the application of the model on either side a straightforward process. We ran a series of comparisons, each consisting of two simulations using identical system designs and weather files. One simulation included the snow model that ran during the SAM PV simulation (on the DC side) and the other simulation included the snow model that ran after the SAM PV simulation (on the AC side). In all cases, the final annual energy values predicted by the two simulations were within 2% of each other, which is within an acceptable error margin. This suggests that the side to which the snow model is applied is not of great importance. Nevertheless, users should be aware that slight differences are expected, particularly if they wish to post-process PV performance data obtained elsewhere using SAM's snow loss model. Unless otherwise specified, it should be assumed that the snow model was applied on the DC side for the remaining analyses discussed in this work.

Error Reduction Demonstration

Snow models have been available to the PV industry for close to two decades; however, in most cases there has not been a large validation effort. User confidence in the conclusions reached using a snow model may increase with greater similarity between the user's system and the system, or systems, from which the snow model was developed, but this is not equivalent to systematic validation. Naturally, a complete validation of a snow model would require comparing simulation results to measured data sets for representatives of each type of system design in each type of weather climate—an effort which is far beyond the scope of this study even if such data sets existed. Nevertheless, in order to build confidence in the results reported by the PV snow coverage model implemented in SAM, we demonstrated the model's effectiveness in reducing the error in estimating annual energy production with respect to measured data for three systems. None of these validation systems played a role in Marion's original model's conception.

Fixed-Tilt Systems

Two of the systems that were used for validation were the Forrestal system, located on the James Forrestal Building in Washington, D.C., and the RSF2 system, located on NREL's Research Support Facility in Golden, Colorado. Both are fixed-tilt systems, with tilt angles of 0° and 10° respectively, that have previously been used as case studies for SAM validations. These validations showed good agreement with SAM predictions excluding system downtime and time periods with heavy snowfall (Freeman et al. 2013). The concurrent weather data and measured data for the two systems come from the same data set used in Freeman et al. (2013); Nov. 2009 - Jul. 2010 for the Forrestal system and 2012 for the RSF2 system.

The results of the snow model validation study are shown in Figure 2. For each month in a year, the figure shows SAM's predicted energy output using the snow model in blue, the actual measured output of the system in green, and SAM's predicted energy output when not using the snow model in red. The number of hours within each month that have a snow coverage percentage above zero, as calculated by the snow model, is displayed above the bars. Each system had several days of down-time, measurement failure, or missing data. For instance, there are no measured data for the Forrestal system spanning the entire months of August, September, and October. The Forrestal system is also missing 7 days of data in mid-July as well as the first 13 days of November, which is why these months display less power output than would be expected during these times. The RSF2 system fares better in the sense that the measured data are only missing 38 days throughout the year. Twenty-two of these missing days occur in the month of July and the remaining 16 are distributed sporadically throughout the year. For our analysis, if the measured data were missing or were otherwise flagged as erroneous for a particular time period, then the simulated outputs for that time period were ignored and weren't factored into error calculations.

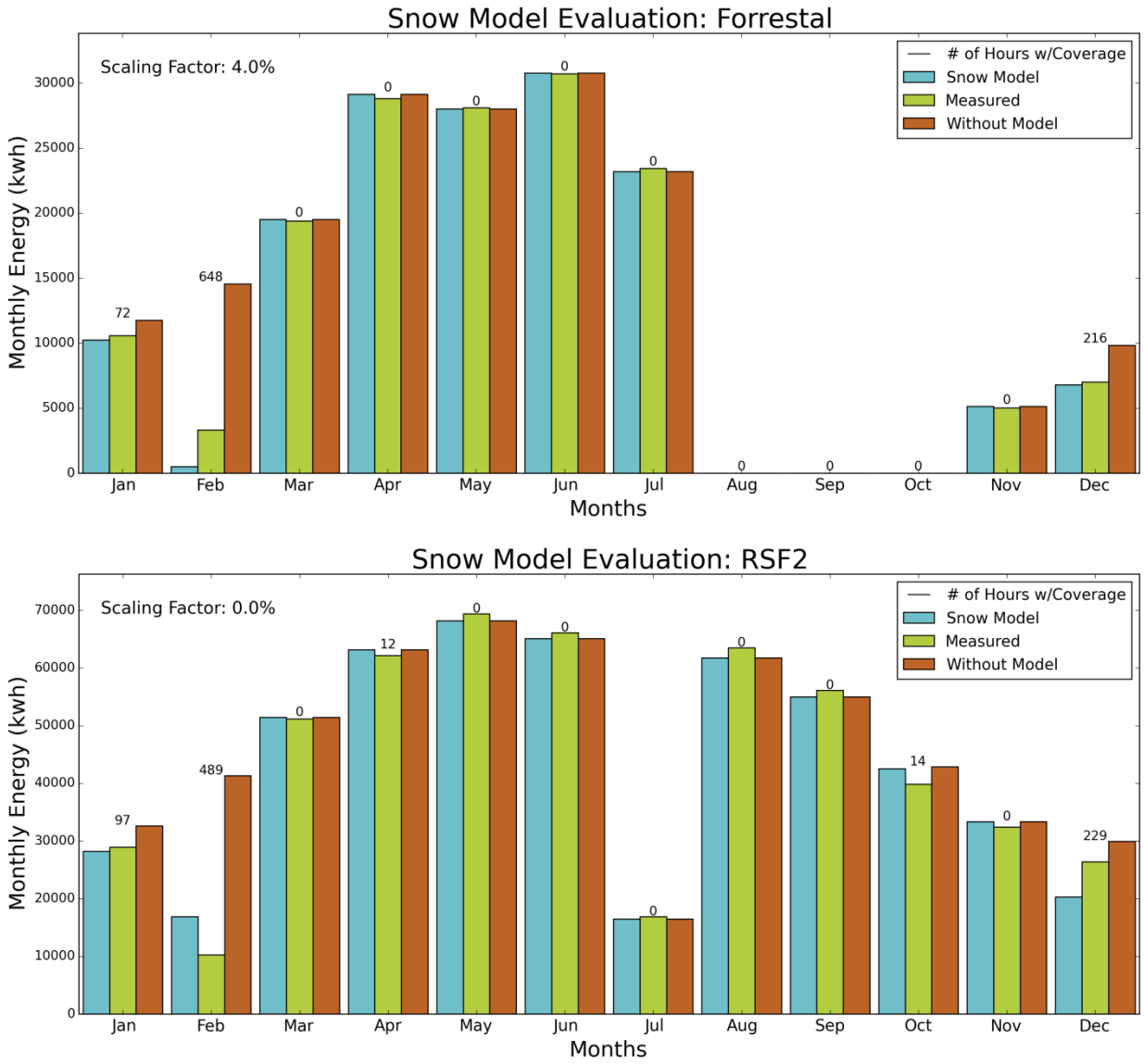

Figure 2. Results from the validation study using the Forrestal system in Washington, D.C. and the RSF2 system in Golden, Colorado

Fortunately, very few of the missing days occur during the months with heaviest snowfall (January, February, and December). Before error calculations were made, however, a scaling factor was applied to the results of each simulation in order to provide the best fit to the measured data during the summer months (April – Aug) and these values are displayed in the top-left corner of each plot of Figure 2. This was done in order to help isolate any error changes which resulted from activating the snow model, rather than having this error skewed by systematic error that is present year-round. Table 1 displays the errors compared to measured data associated with each of the winter months, as well as the errors in total annual energy. Error calculations were performed using:

$$Error = \frac{Simulated - Measured}{Measured} \times 100\%$$

Reductions in absolute annual error were also included in order to provide a sense of how changes in each particular month affected the total annual error. These values are calculated using:

$$Abs.\,Annual\ Error\ Red. = \frac{(\,|Without\ Model| - |With\ Model|\,) * Measured\ Monthly\ Energy}{Measured\ Annual\ Energy}$$

In Table 1, positive error values correspond to an over-prediction of the estimated energy production, while negative values indicate an under-prediction. A decrease in the absolute value of these error percentages, reported as a positive value in the 'Absolute Annual Error Reduction' row, reflects an improvement in the simulation's annual prediction, because the estimated energy production with the snow model activated is closer to the measured production. In the majority of cases, the snow model is observed to significantly improve the monthly estimated energy. December of the RSF2 system is the only exception to this, which will be discussed below. For both systems, the month of February contributed most to annual error before the snow model was employed, and likewise showed a huge improvement in energy production estimations—improving the total annual error by close to 5% in each case. Most importantly, the snow model is observed to greatly improve SAM's post-scaling factor estimate in annual energy in both cases: from total absolute annual error of 9.9% to 1.9% for the Forrestal system and from 7.3% to 0.1% for the RSF2 system.

Table 1. Monthly and Annual Errors With and Without Snow Model

		January	February	December	Annual
Forrestal	With Model (%)	-2.9	-85.0	-3.0	-1.9
	Without Model (%)	11.3	337.6	40.4	9.9
	Absolute Annual Error Reduction (%)	0.6	5.4	1.7	8.0
RSF2	With Model (%)	-2.4	64.3	-23.2	-0.1
	Without Model (%)	12.7	302.1	13.4	7.3
	Absolute Annual Error Reduction (%)	0.6	4.7	-0.5	7.2

The snow model is observed to both over-predict and under-predict energy estimates in an unforeseeable fashion on a monthly, daily, or hourly basis. This is expected behavior, however, since Marion et al. (2013) states that the original model performs well on an annual average despite the fact that "large differences between modeled and measured energy losses should be expected for monthly or shorter time periods" (119). For this reason, results from the model implemented in SAM should only be factored into annual considerations and not applied to monthly or shorter time periods.

One-Axis Tracking Systems

Sun tracking systems are believed to be much less affected by snow coverage than fixed-tilt systems due to the vibrations and movements of the panels. Nevertheless, the ability to estimate snow losses on tracking systems, however slight they may be, is a recognized need. Because it does not address any potential effects of system movement, Marion's PV snow coverage model was originally only intended for fixed-tilt systems, so we investigated the implemented model's efficacy when applied to tracking systems. Unfortunately, we did not have measured data for a two-axis tracking system, but we were able to apply our model to a one-axis tracking system: the Mesa Top PV array located in Golden Colorado. The measured data and system specifications were also taken from the work by Freeman et al. (2013). This was the third system used in our validation study and the results of this work are shown in Figure 3, while the associated errors are included in Table 2.

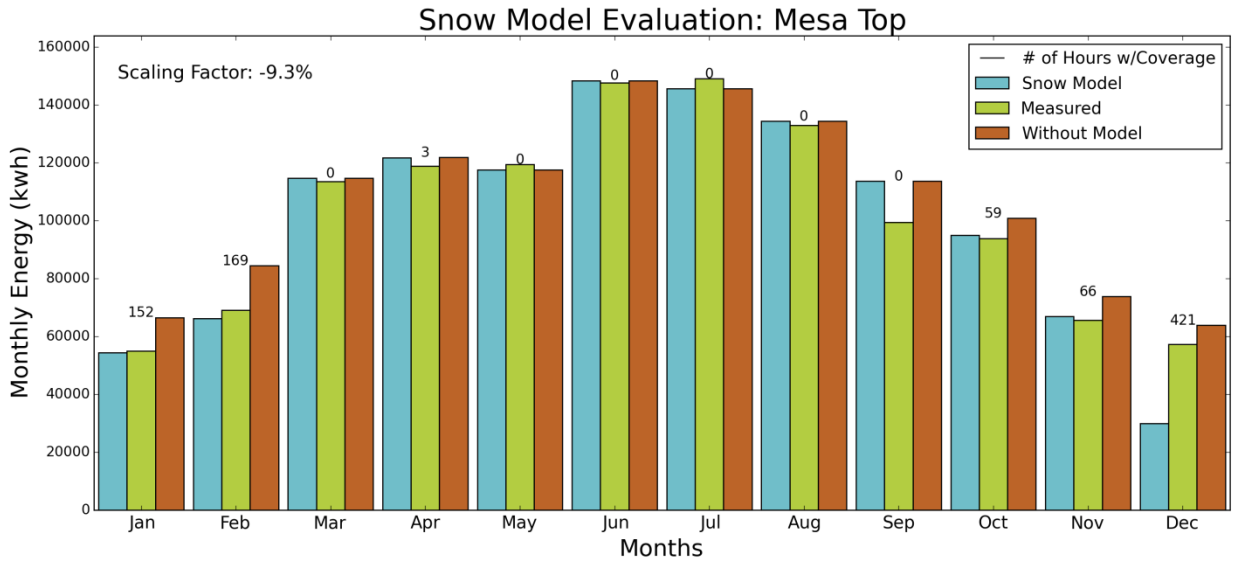

Figure 3. Results from applying the implemented snow model to the Mesa Top one-axis tracking array in Golden, Colorado

Like the fixed-tilt systems, the Mesa Top simulations showed significant improvement when the snow model was activated to post-scaling factor simulations, reducing the annual energy estimation error from 5.2% to 1.1%. It can be seen in Figure 3, however, that a large portion of the annual error, both with and without the snow model, comes from September— a month with no measured snowfall. At this time we are unsure of the cause of the discrepancy observed in September; however, in order to isolate changes in error resulting from using the snow model, we can artificially lower the simulation's output in September to the measured value. By doing so, and recalculating the annual errors, we find that the annual error without activating the snow model would be 4.1% while the annual error with activating the snow model would be -2.3%. Both methods of calculating the annual error are reported in Table 2. While this still represents an improvement in the annual energy predictions, the improvement is not nearly as much as was observed for the fixed-tilt systems. Moreover, it is clear that the snow model is over-predicting snow losses in December by a large margin. As previously mentioned, this observation is likely

due to the fact that the snow model does not account for snow removal resulting from movement of the array's panels, which likely speeds the snow removal process. Nevertheless, with the exception of December, the snow model is observed to significantly improve SAM's energy production estimates for months with snowfall. These results build confidence that the snow model implemented in SAM can help reduce annual prediction error for tracking systems.

Table 2. Monthly and Annual Errors With and Without Snow Model

		January	February	October	November	December	Annual	Annual altered September
Mesa Top	With Model (%)	-1.0	-4.1	1.2	1.8	-47.7	-1.1	-2.3
	Without Model (%)	21.0	22.3	7.6	12.3	11.6	5.2	4.1
	Absolute Annual Error Reduction (%)	0.9	1.0	0.5	0.6	-1.7	4.1	1.9

This study also estimated the effect of nighttime system position on annual energy output. Most single-axis tracking systems, including the Mesa Top system, are kept in a "stow" position overnight. This means that the rows (Figure 1) are positioned such that average wind loads are minimized, which, for the Mesa Top system, amounts to a nighttime tilt of 5° to the east. Lower tilt angles inhibit snow removal by sliding, which is likely the only active snow removal process during the night. By instructing the simulation of the Mesa Top system to set the nighttime tilt angle to 20° instead of 5°, we found that the simulated system would produce an estimated 19,800 kWh of additional energy over the course of the year, a 1.49% increase, as a direct result of snow sliding during the night. This suggests that an analysis of the empirical effect of increasing the tilt angle of the nighttime stow position in response to expected snowfall could quantify an increase in tracking system energy production.

National Study

Following the validation exercises, we applied the snow model to a wide variety of locations in order to estimate typical trends in PV snow coverage losses across the continental United States. In order to accomplish this, we constructed two common system designs in SAM and then used the 1961-1990 NSRDB data set— the underlying historical data used to produce the NSRDB's TMY2 data set. This data set is comprised of hourly meteorological weather data (including daily snow depth measurements) for 239 locations across the United States, spanning the years of 1961 through 1990. For each of the two system types, two simulations were conducted for every year at each location: one without the snow model activated as well as one with the snow model activated, and a percent difference was calculated.

The system designs we used assume the tilt-equals-latitude and tilt-equals-20° conventions, both of which are common designs in the PV industry. In the first case, not only is it thought that setting the tilt angle of a fixed-tilt PV array to the latitude of its location will maximize the total solar radiation over a single year (ignoring shading effects of the surrounding environment), but also, since snowy climates are generally found in the northern areas of the country, the larger tilt angles at these locations are expected to promote quicker snow removal, thereby mitigating the array's losses from snow coverage. On the other hand, system tilts of 20° are found fairly commonly in the industry due to the simplicity and common availability of this system design. Beyond setting tilt angles to either the latitude or 20° for each simulation, however, all other parameters have been left as the SAM defaults for the detailed photovoltaic/ no financial model in version 2015.1.30. This facilitates replication and avoids listing the many input parameters required by SAM's pvsamv1 compute module. The results of this study are displayed in Figure 4.

Figure 4 shows the average percent loss in PV production due to snow coverage over the thirty years at each of the TMY2 sites for both system designs (see Appendix for full data). For both system designs, most PV snow loss is concentrated in an area beginning in the Northeast, spanning the Great Lakes, and continuing into the Midwest and Rocky Mountain regions (particularly in Wyoming). This general trend was certainly an expected outcome of this study; however, it is still surprising to see that PV arrays in these areas might experience losses between 15- 25% of their total available energy output. It is also surprising to see that areas which are not generally associated with snow, such as eastern Nevada, might also see losses between 5-10% of their annual PV energy production. There are pockets within the Rocky Mountain and Southwest regions, located in high altitude areas, which are estimated to suffer from much higher annual losses than the surrounding regions. One instance of this, Flagstaff, Arizona, was estimated to lose an average of 12% of its total annual energy to snow coverage while its closest neighbor, Phoenix, Arizona, was only estimated to lose 2%.

The most unexpected outcome of this study, however, is certainly the fact that 20° tilt systems actually showed slightly lower losses on a percentage basis compared against tilt-equals-latitude systems at almost all locations, contrary to our initial hypothesis. This may be due to the fact that, even though the 20° systems likely suffer a higher percentage of monthly snow loss in the winter months compared to their tilt-equals-latitude counterparts, the benefit of lower tilt angles during the summer is enough to overcome this effect. Of course, these maps only display the average percent loss at each location and say nothing about the total annual production of either

system. In general, even when accounting for snow coverage, the tilt-equals-latitude systems were still observed to produce more annual energy than their 20° tilt counterparts.

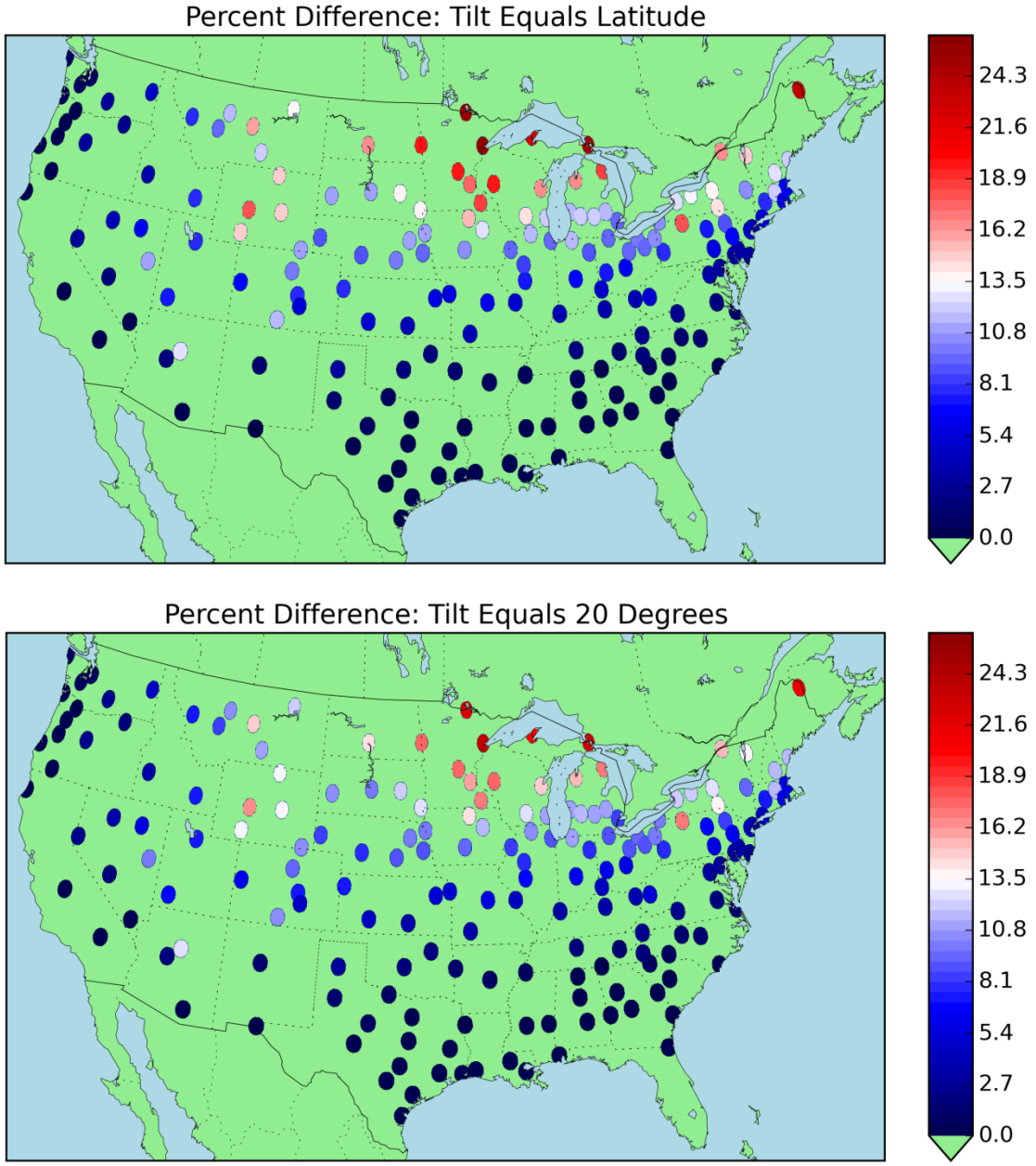

Figure 4. Results from a national study modeling PV production losses due to snow coverage using both a fixed-tilt tilt-equals-latitude and a constant 20° tilt system design, the historical TMY2 data set, and the newly implemented snow model in SAM

Note: The values displayed at each of the data sites in this study were found by determining, for each individual year and system type, the difference between the results of a simulation without the snow model activated and a simulation with the snow model activated. Then an average and standard deviation of these differences were calculated from the 30 years at each of the locations. Finally, each location was normalized by the average of the values without the snow model activated in order to isolate the effects of the snow losses as a percentage.

From observations based on Figure 4, we have constructed general trends in snow losses across the United States. Figure 5 displays these results. This map can be utilized as a starting point for snow loss estimations for PV systems where better snow loss information is unavailable. For instance, if a PV system is to be built in western Kansas and a simulation, which does not account for snow, of this system estimated that it would produce 8,000 kWh annually, then this figure indicates that the designer might also want to include a 4% to 10% loss attributed to snow. It is important to note, however, that these values may not be representative of any particular year, nor do they account for any microclimates that might be present. Rather, these values are only meant to represent a starting point for estimating snow losses in a given area before a more specialized analysis can be performed. If measured snow depth data is available for a given location or year being analyzed, it would certainly be beneficial to simulate the PV system using the measured snow depth data instead of simply using the loss indicated in Figure 5.

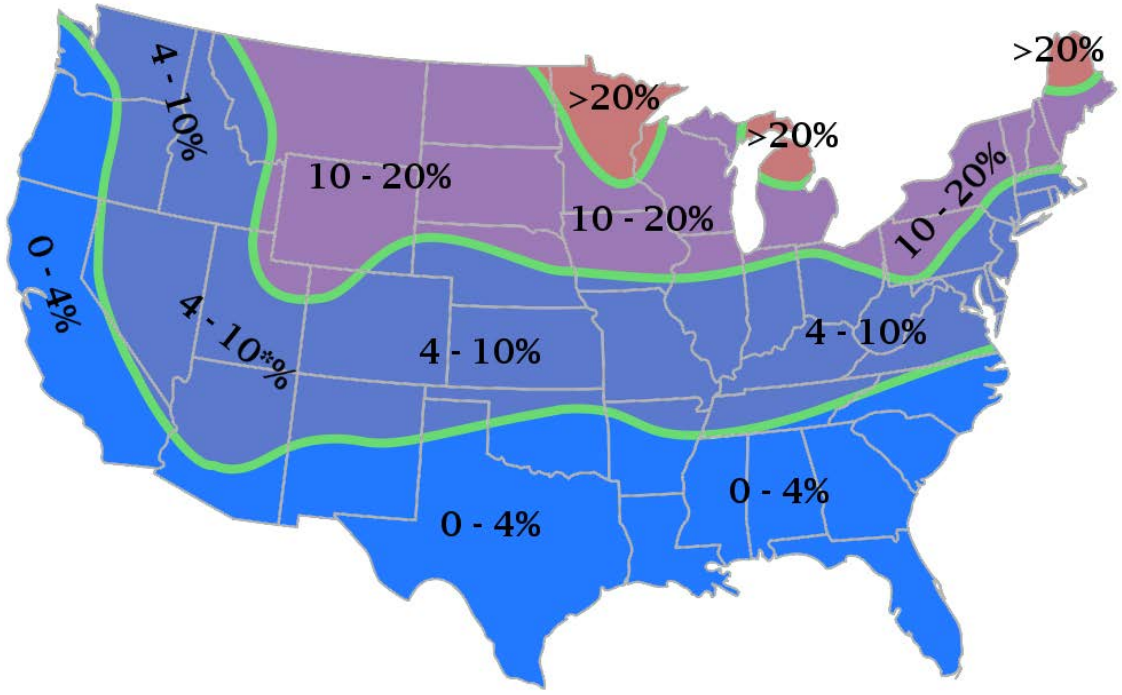

Figure 5. General trends in average snow losses as a percentage of annual energy production

Note: Like-colored regions have similar loss percentages and are labeled in the figure. The specific region around Nevada and the Four Corners states is special (indicated by an *) in that high altitude regions, such as Flagstaff, Arizona and Ely, Nevada should be considered to be in the next higher tier of snow losses. This plot is a broad enough generalization that it may apply to either a tilt=latitude or a tilt=20° system.

Finally, by sorting simulation results based on snow depth rather than geographic location, we were also able to find an interesting correlation between total snow depth throughout a year and the total percent loss resulting from snow coverage for the tilt-equals-latitude systems. The results of this are displayed in Figure 6. This figure uses the sum of hourly snow depths, found using:

$$S(h) = \sum_{i=0}^{h} \text{snow\_depth}[i]$$

where S indicates the sum of hourly snow depths, h indicates the hour in the year, and $\text{snow\_depth}[i]$ refers to the measured snow depth at the i^{th} hour. This quantity takes into account both the total snowfall throughout the course of a year as well as snow persistence during that year. The percent loss reported for each simulation was calculated in the same manner as it was for Figure 4: by subtracting the result of the simulation with the snow model activated from the result of the simulation without the snow model activated, followed by normalizing this number by the latter. Figure 6 shows a predictable trend in which more snow depth throughout a year corresponds to higher percent loss. A fit for this data is shown in the figure; the spread of the percent loss at each summed snow depth value is generally observed to be close to ±50% of the fitted curve's value at that point.

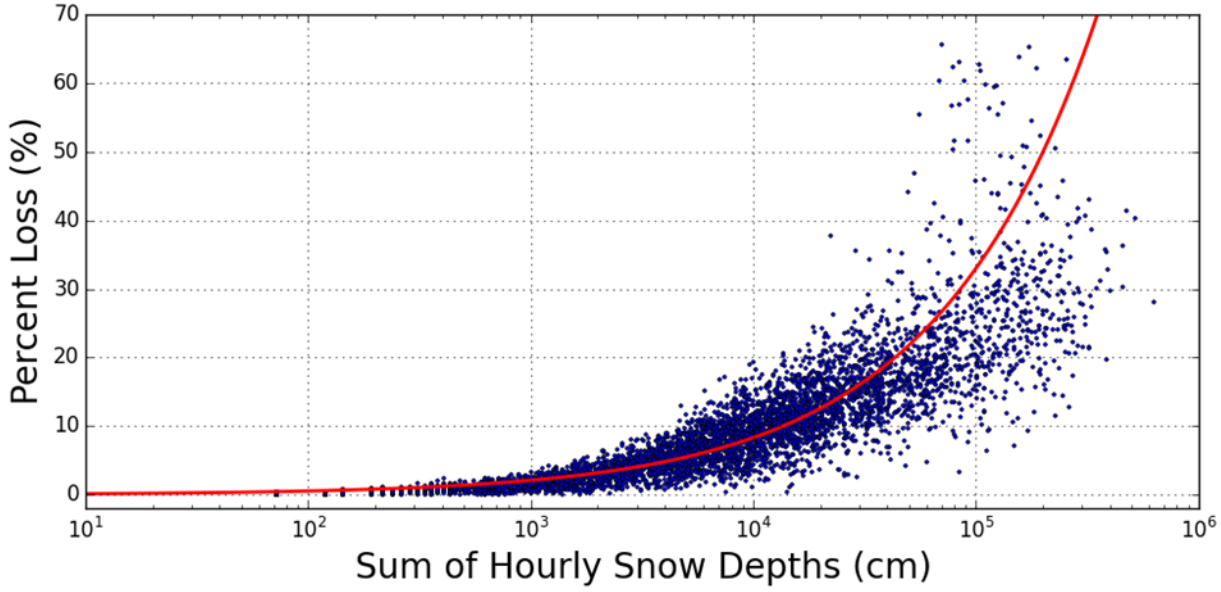

Figure 6. Correlation between the sum of the hourly snow depth array and the resulting percent loss for each year of each location in the tilt-equals-latitude national study

Conclusions and Future Work

For several years, the PV community has expressed a need for a reliable model that estimates losses in PV energy production resulting from snow coverage. In an effort to fill this void, we have implemented a snow model into SAM and demonstrated its effectiveness against two fixed-tilt systems and a one-axis tracking system, none of which were a part of the model's original development. Subsequently, we conducted a nationwide study to estimate national trends in snow loss percentages to serve as a starting point for more accurate modeling of PV production in snowy areas.

The final implemented PV snow coverage model was kept as similar as possible to Marion's original model (Marion et al. 2013). A few changes were necessary, however, in order to prevent illogical behavior of the model when implemented in SAM, as well as to accommodate for hourly and sub-hourly simulations. We showed that the model could be applied on either the DC or the AC side of power conversion with very little effect (<2%) on the resulting energy estimates. During our validation study, we observed that our implemented model decreased the estimated annual energy error (in comparison to measured values) by over 75% for the fixed-tilt systems and by 36% for the tracking system. These represent significant improvements to SAM's performance in snowy conditions and, as a result, we are confident the snow model will provide meaningful snow loss estimations to SAM users. In this analysis, we also discovered that increasing the tilt angles of tracking systems during the night may have the potential to slightly increase the annual energy production of these systems by allowing snow to slide off more easily.

Our national study agreed with previous studies that PV snow coverage losses for fixed-tilt systems range from 0% to 25%, which is summarized in a map of general estimated snow loss trends across the continental United States. The results from this study can potentially be used as a starting point for future predictions of PV snow losses in these areas. Lastly, we were also able to produce a correlation between total snow depth over a year and the percent loss for fixed-tilt, tilt-equals-latitude systems, which could also be a good starting point for snow loss estimations if a user has access to snow depth data.

There are certainly areas for improvement in the snow model. It has been shown to improve energy predictions on an annual scale, but the model can both over-predict or under-predict snow losses for any given hour, day, or month (Figure 2). Any effort to reduce these variations will do much to further improve upon the model's accuracy. This could mean incorporating snow removal processes other than sliding, such as melting and wind removal. Another possible improvement would be to investigate whether or not the sliding coefficient discussed in the implementation section is a function of snow consistency or module temperature. Additionally, the model does not account for time-delayed effects, such as a particularly cold night freezing the bottom layer of snow onto a PV array and preventing sliding during the day. Lastly, although we demonstrated the model's efficacy against three independent systems, this model will certainly not always produce reliable results for any PV system in any location. As measured data sets for other systems in snowy areas become available, we hope to continue validation of this snow model with additional systems.

In the meantime, we hope that this tool will allow the PV community to make more accurate annual energy estimates for systems in all areas of the United States, particularly in the areas which are heavily affected by snow, thereby encouraging more informed technical and financial decisions in the development of future PV systems.

References

Marion, B.; Schaefer, R.; Caine, H.; Sanchez, G. (2013). "Measured and modeled photovoltaic system energy losses from snow for Colorado and Wisconsin locations." *Solar Energy* 97; pp. 112-121.

Becker, G.; Schiebelsberger, B.; Weber, W.; Vodermayer, C.; Zehner, M.; Kummerle, G. (2006). "An approach to the impact of snow on the yield of grid-connected PV systems." *Proc. European PVSEC*.

Powers, L.; Newmiller, J.; Townsend, W. (2010). "Measuring and modeling the effect of snow on photovoltaic system performance." Presented at Photovoltaic Specialists Conference (PVSC).

Andrews, R.W.; Pollard, A.; Pearce, J.M. (2013). "A new method to determine the effects of hydrodynamic surface coatings on the snow shedding effectiveness of solar photovoltaic modules." *Solar Energy Materials and Solar Cells* 113; pp. 71-78.

Sugiura, T.; Yamadaa, T.; Nakamuraa, H.; Umeyaa, M.; Sakutab, K.; Kurokawa, K. (2003). "Measurements, analyses and evaluation of residential PV systems by Japanese monitoring program." *Solar Energy Materials and Solar Cells* 73(3); pp. 767-779.

Townsend, T.; Powers, L. (2011). "Photovoltaics and snow: An update from two winters of measurements in the sierra." in PVSC.

Andrews, R.W.; Pearce, J.M. (2012). "Prediction of energy effects on photovoltaic systems due to snowfall events." Presented at PVSC .

Freeman, J.; Whitmore, J.; Kaffine, L.; Blair, N.; Dobos, A.P. (2013). "System Advisor Model: Flat plate photovoltaic performance modeling validation report." NREL/TP-6A20-60204. Golden, CO: National Renewable Energy Laboratory. Accessed April 2015: http://www.nrel.gov/docs/fy14osti/60204.pdf.

"National Solar Radiation Data Base: 1961- 1990: Typical Meteorological Year 2." NSRDB (1995). Accessed March 2015: http://rredc.nrel.gov/solar/old_data/nsrdb/1961-1990/tmy2/.

Appendix

Tabulated results from tilt-equals-latitude study

Locations whose losses are listed as a dash (-) were unable to be simulated in this study and do not reflect a calculation of zero snow loss for that location.

City	State	Average Percent Loss	STD Percent Loss	City	State	Average Percent Loss	STD Percent Loss
Abilene	TX	0.7	0.7	Lander	WY	18	4.6
Akron	OH	9.7	2.6	Lansing	MI	12.2	2.7
Alamosa	CO	11.8	5.5	Las Vegas	NV	0	0.2
Albany	NY	10.4	3.9	Lewistown	MT	13.4	6.6
Albuquerque	NM	1.6	1.1	Lexington	KY	3.7	2.6
Allentown	PA	6.6	3	Lihue	HI	0	0
Alpena	MI	18.6	4	Little Rock	AR	0.7	0.7
Amarillo	TX	3	1.7	Long Beach	CA	-	-
Anchorage	AK	14.8	6.1	Los Angeles	CA	0	0
Annette	AK	2.5	2.1	Louisville	KY	-	-
Arcata	CA	0	0.1	Lubbock	TX	1.6	1.1
Asheville	NC	2	1.4	Lufkin	TX	0.1	0.2
Astoria	OR	0.3	0.6	Lynchburg	VA	-	-
Athens	GA	-	-	Macon	GA	0.1	0.3
Atlanta	GA	0.2	0.3	Madison	WI	14.3	4.1
Atlantic City	NJ	2.7	1.8	Mansfield	OH	9.7	2.8
Augusta	GA	0.2	0.3	Mason City	IA	15.6	5.5
Austin	TX	0.1	0.3	Massena	NY	16.7	4.3
Bakersfield	CA	0	0	Mcgrath	AK	26.9	6.7
Baltimore	MD	3	2	Medford	OR	0.3	0.5
Barrow	AK	55.9	10.2	Memphis	TN	0.8	0.9
Baton Rouge	LA	0	0.1	Meridian	MS	0.2	0.4
Bethel	AK	25.5	9.3	Miami	FL	0	0
Bettles	AK	33.8	5.2	Midland	TX	-	-
Big Delta	AK	25.8	6.3	Miles City	MT	-	-
Billings	MT	12.2	3.7	Milwaukee	WI	12.4	4
Binghamton	NY	14.5	2.8	Minneapolis	MN	17.7	4.9
Birmingham	AL	0.2	0.3	Minot	ND	-	-
Bismarck	ND	16.5	4.8	Missoula	MT	7.8	3.1
Boise	ID	3.7	3	Mobile	AL	0.1	0.2
Boston	MA	6	2.4	Moline	IL	9.4	3.8
Boulder	CO	10.1	2.7	Montgomery	AL	0.1	0.2
Bradford	PA	18.1	2.3	Muskegon	MI	11.4	2.8
Bridgeport	CT	5.1	2.4	Nashville	TN	1.8	1.4
Bristol	TN	2.7	1.6	New Orleans	LA	0	0.1
Brownsville	TX	0	0	New York City	NY	3.7	1.9
Buffalo	NY	12.9	2.6	Newark	NJ	4.4	2.1
Burlington	VT	15.1	4.6	Nome	AK	31.3	8.9
Burns	OR	-	-	Norfolk	NE	11.3	4
Cape Hatteras	NC	0.2	0.4	Norfolk	VA	1.1	1.2
Caribou	ME	23.6	4.5	North Bend	OR	0.1	0.4
Casper	WY	15	3.6	North Platte	NE	8.8	3.6
Cedar City	UT	7.4	3.5	Oklahoma City	OK	1.8	1.5
Charleston	SC	-	-	Olympia	WA	0.9	1.2
Charleston	WV	5.2	2.3	Omaha	NE	9.7	3.7
Charlotte	NC	0.8	0.6	Pendleton	OR	2.4	1.9
Chattanooga	TN	0.5	0.5	Peoria	IL	8.3	4
Cheyenne	WY	11	3	Philadelphia	PA	3.5	2
Chicago	IL	9.5	3.6	Phoenix	AZ	0	0
Cleveland	OH	10	2.5	Pierre	SD	11.1	4.3
Cold Bay	AK	12.1	4.8	Pittsburgh	PA	8.1	2.8
Colorado Springs	CO	4.4	3.9	Pocatello	ID	8	3.5
Columbia	MO	6	2.3	Port Arthur	TX	0	0.1
Columbia	SC	0.2	0.4	Portland	ME	12.4	3.1
Columbus	GA	0.1	0.2	Portland	OR	0.3	0.4
Columbus	OH	6.2	3.3	Prescott	AZ	1.9	1.5

City	State	Average Percent Loss	STD Percent Loss	City	State	Average Percent Loss	STD Percent Loss
Concord	NH	12.6	3.5	Providence	RI	5.9	2.3
Corpus Christi	TX	0	0	Pueblo	CO	5.1	2.5
Covington	KY	5	3.3	Quillayute	WA	0.8	1.2
Cut Bank	MT	-	-	Raleigh	NC	1.2	1
Daggett	CA	0	0.1	Rapid City	SD	11.3	3.8
Dayton	OH	7	3.5	Redmond	OR	2.8	1.4
Daytona Beach	FL	0	0	Reno	NV	2.8	1.7
Des Moines	IA	10.7	4	Richmond	VA	2.1	1.4
Detroit	MI	9.2	3.3	Roanoke	VA	2.2	1.7
Dodge City	KS	5.1	2.2	Rochester	MN	18.8	5.5
Duluth	MN	26.5	5	Rochester	NY	13	2.3
Eagle	CO	-	-	Rock Springs	WY	14	5
Eau Claire	WI	19.5	4.8	Rockford	IL	11.7	4.4
El Paso	TX	0.5	0.7	Sacramento	CA	0	0
Elkins	WV	-	-	Saint Cloud	MN	19.7	5.6
Elko	NV	6.1	3.7	Salem	OR	0.4	0.8
Ely	NV	11.3	4.5	Salt Lake City	UT	7.7	3.3
Erie	PA	10.7	2.4	San Angelo	TX	0.4	0.3
Eugene	OR	0.5	0.8	San Antonio	TX	0.1	0.2
Evansville	IN	3.8	2.6	San Diego	CA	0	0
Fairbanks	AK	24.9	5.9	San Francisco	CA	0	0
Fargo	ND	19.9	6.4	San Juan	PR	0	0
Flagstaff	AZ	11.9	4.5	Santa Maria	CA	0	0
Flint	MI	11.8	2.8	Sault Ste. Marie	MI	25.4	4.9
Fort Smith	AR	1.2	1.4	Savannah	GA	0.1	0.3
Fort Wayne	IN	8.9	3.2	Scottsbluff	NE	8.9	1.9
Fort Worth	TX	0.5	0.6	Seattle	WA	0.6	1
Fresno	CA	0	0	Sheridan	WY	14.7	3.4
Glasgow	MT	13.8	5.5	Shreveport	LA	0.3	0.5
Goodland	KS	7.8	2.5	Sioux City	IA	10.9	4.3
Grand Island	NE	9.8	3.8	Sioux Falls	SD	13.8	5
Grand Junction	CO	7	3.8	South Bend	IN	11.9	3
Grand Rapids	MI	12.4	3.1	Spokane	WA	4.8	2.8
Great Falls	MT	11.8	4.1	Springfield	IL	7.2	3.2
Green Bay	WI	16.4	4.4	Springfield	MO	3.9	1.8
Greensboro	NC	1.4	1.1	St Paul Is.	AK	20.1	11
Greenville	SC	0.6	0.5	St. Louis	MO	5.2	2.8
Guam	PI	0.2	0	Sterling	VA	3.3	1.9
Gulkana	AK	23.1	5.6	Syracuse	NY	13.9	2.7
Harrisburg	PA	5.6	2.7	Talkeetna	AK	20.4	7.2
Hartford	CT	8.1	2.7	Tallahassee	FL	0	0
Helena	MT	9.6	3.9	Tampa	FL	0	0
Hilo	HI	0	0	Toledo	OH	9.5	3.2
Honolulu	HI	0	0	Tonopah	NV	1.8	1.2
Houghton	MI	16.9	9.3	Topeka	KS	5.5	2.7
Houston	TX	0	0.1	Traverse City	MI	16.4	3.3
Huntington	WV	4	2.3	Tucson	AZ	0.1	0.1
Huntsville	AL	0.5	0.6	Tucumcari	NM	-	-
Huron	SD	13.9	4.6	Tulsa	OK	2	1.5
Indianapolis	IN	6.6	3.3	Victoria	TX	0	0.1
International Falls	MN	25.7	5.6	Waco	TX	0.2	0.3
Jackson	MS	0.2	0.4	Waterloo	IA	12.7	4.7
Jacksonville	FL	0	0.1	West Palm Beach	FL	0	0
Kahului	HI	0	0	Wichita Falls	TX	1	1
Kalispell	MT	-	-	Wichita	KS	4	2.3
Kansas City	MO	4.7	3.1	Wilkes-barre	PA	8.9	3
Key West	FL	0	0	Williamsport	PA	7.4	2.8
King Salmon	AK	15.3	8	Wilmington	DE	3.6	2.2
Knoxville	TN	1.5	1.2	Wilmington	NC	0.3	0.5
Kodiak	AK	7.7	4.7	Winnemucca	NV	4.1	2.9
Kotzebue	AK	38	7.9	Worchester	MA	12.3	4.3
La Crosse	WI	-	-	Yakima	WA	2.8	1.6
Lake Charles	LA	0	0.1	Yakutat	AK	14.1	6.4
				Youngstown	OH	10.6	2.8

Tabulated results from 20° tilt study

Locations whose losses are listed as a dash (-) were unable to be simulated in this study and do not reflect a calculation of zero snow loss for that location.

City	State	Average Percent Loss	STD Percent Loss	City	State	Average Percent Loss	STD Percent Loss
Abilene	TX	0.7	0.6	Lander	WY	16.6	4.4
Akron	OH	8.9	2.4	Lansing	MI	11.3	2.5
Alamosa	CO	10.6	4.9	Las Vegas	NV	0	0.1
Albany	NY	9.5	3.5	Lewistown	MT	14.7	3.7
Albuquerque	NM	1.5	1	Lexington	KY	3.5	2.4
Allentown	PA	6.1	2.7	Lihue	HI	-	-
Alpena	MI	17	3.5	Little Rock	AR	0.6	0.7
Amarillo	TX	2.8	1.6	Long Beach	CA	-	-
Anchorage	AK	-	-	Los Angeles	CA	0	0
Annette	AK	-	-	Louisville	KY	-	-
Arcata	CA	0	0.1	Lubbock	TX	1.5	1.1
Asheville	NC	1.9	1.3	Lufkin	TX	0.1	0.2
Astoria	OR	0.3	0.5	Lynchburg	VA	-	-
Athens	GA	-	-	Macon	GA	0.1	0.2
Atlanta	GA	0.2	0.3	Madison	WI	12.9	3.7
Atlantic City	NJ	2.6	1.6	Mansfield	OH	8.9	2.5
Augusta	GA	0.2	0.3	Mason City	IA	14.1	5
Austin	TX	0.1	0.3	Massena	NY	15.3	3.9
Bakersfield	CA	0	0	Mcgrath	AK	-	-
Baltimore	MD	2.8	1.8	Medford	OR	0.3	0.4
Barrow	AK	-	-	Memphis	TN	0.8	0.9
Baton Rouge	LA	0	0.1	Meridian	MS	0.2	0.3
Bethel	AK	-	-	Miami	FL	0	0
Bettles	AK	-	-	Midland	TX	-	-
Big Delta	AK	-	-	Miles City	MT	-	-
Billings	MT	10.8	3.3	Milwaukee	WI	11.2	3.6
Binghamton	NY	13.5	2.5	Minneapolis	MN	15.9	4.6
Birmingham	AL	0.2	0.3	Minot	ND	-	-
Bismarck	ND	14.5	4.3	Missoula	MT	7.1	2.8
Boise	ID	3.3	2.5	Mobile	AL	0.1	0.2
Boston	MA	5.7	2.1	Moline	IL	8.5	3.4
Boulder	CO	9.4	2.4	Montgomery	AL	0.1	0.2
Bradford	PA	16.8	2.1	Muskegon	MI	10.9	2.6
Bridgeport	CT	4.8	2.2	Nashville	TN	1.7	1.3
Bristol	TN	2.5	1.5	New Orleans	LA	0	0.1
Brownsville	TX	0	0	New York City	NY	3.5	1.8
Buffalo	NY	11.9	2.3	Newark	NJ	4.1	1.8
Burlington	VT	13.8	4	Nome	AK	-	-
Burns	OR	-	-	Norfolk	NE	10.1	3.7
Cape Hatteras	NC	0.2	0.4	Norfolk	VA	1.1	1.1
Caribou	ME	21.4	3.9	North Bend	OR	0.1	0.4
Casper	WY	13.4	3.2	North Platte	NE	8	3.3
Cedar City	UT	7	3.2	Oklahoma City	OK	1.7	1.4
Charleston	SC	-	-	Olympia	WA	0.8	1
Charleston	WV	4.9	2.1	Omaha	NE	8.8	3.4
Charlotte	NC	0.8	0.6	Pendleton	OR	2.1	1.6
Chattanooga	TN	0.5	0.5	Peoria	IL	7.6	3.6
Cheyenne	WY	10.3	2.8	Philadelphia	PA	3.3	1.9
Chicago	IL	8.6	3.1	Phoenix	AZ	0	0
Cleveland	OH	9.2	2.2	Pierre	SD	10	4
Cold Bay	AK	-	-	Pittsburgh	PA	7.6	2.6
Colorado Springs	CO	7.1	2.9	Pocatello	ID	7.4	3.5
Columbia	MO	5.6	2.2	Port Arthur	TX	0	0.1
Columbia	SC	0.2	0.4	Portland	ME	11.5	2.9
Columbus	GA	0.1	0.2	Portland	OR	0.3	0.3
Columbus	OH	5.7	3	Prescott	AZ	1.8	1.3
Concord	NH	11.7	3.3	Providence	RI	5.6	2.2
Corpus Christi	TX	0	0	Pueblo	CO	4.8	2.1
Covington	KY	4.5	3	Quillayute	WA	0.9	1
Cut Bank	MT	-	-	Raleigh	NC	1.1	0.9
Daggett	CA	0	0	Rapid City	SD	10.4	3.6

City	State	Average Percent Loss	STD Percent Loss	City	State	Average Percent Loss	STD Percent Loss
Dayton	OH	6.4	3.2	Redmond	OR	2.4	1.1
Daytona Beach	FL	0	0	Reno	NV	2.6	1.6
Des Moines	IA	9.7	3.8	Richmond	VA	2	1.3
Detroit	MI	8.4	2.9	Roanoke	VA	2.2	1.6
Dodge City	KS	4.7	2	Rochester	MN	16.9	5
Duluth	MN	23.6	4.5	Rochester	NY	12	2
Eagle	CO	-	-	Rock Springs	WY	13.3	4.3
Eau Claire	WI	17.3	4.4	Rockford	IL	10.8	3.8
El Paso	TX	0.5	0.6	Sacramento	CA	0	0
Elkins	WV	-	-	Saint Cloud	MN	17.7	5
Elko	NV	5.7	3.4	Salem	OR	0.4	0.6
Ely	NV	10.2	3.9	Salt Lake City	UT	7.2	3
Erie	PA	9.9	2	San Angelo	TX	0.4	0.3
Eugene	OR	0.4	0.7	San Antonio	TX	0.1	0.2
Evansville	IN	3.5	2.5	San Diego	CA	0	0
Fairbanks	AK	-	-	San Francisco	CA	0	0
Fargo	ND	17.6	5.6	San Juan	PR	-	-
Flagstaff	AZ	12.5	4	Santa Maria	CA	0	0
Flint	MI	10.9	2.5	Sault Ste. Marie	MI	22.8	4.6
Fort Smith	AR	1.1	1.4	Savannah	GA	0.1	0.2
Fort Wayne	IN	8	3	Scottsbluff	NE	8.2	1.8
Fort Worth	TX	0.5	0.6	Seattle	WA	0.5	0.8
Fresno	CA	0	0	Sheridan	WY	13.5	3.3
Glasgow	MT	12.2	4.9	Shreveport	LA	0.3	0.4
Goodland	KS	7.2	2.2	Sioux City	IA	10	4.2
Grand Island	NE	8.8	3.4	Sioux Falls	SD	12.6	4.7
Grand Junction	CO	6.4	3.4	South Bend	IN	10.9	2.8
Grand Rapids	MI	11.6	3	Spokane	WA	4.3	2.5
Great Falls	MT	10.4	3.7	Springfield	IL	6.6	3
Green Bay	WI	14.6	3.9	Springfield	MO	3.7	1.8
Greensboro	NC	1.3	1	St Paul Is.	AK	-	-
Greenville	SC	0.6	0.5	St. Louis	MO	4.8	2.6
Guam	PI	-	-	Sterling	VA	3.2	1.7
Gulkana	AK	-	-	Syracuse	NY	12.8	2.3
Harrisburg	PA	5.4	2.5	Talkeetna	AK	-	-
Hartford	CT	7.5	2.5	Tallahassee	FL	0	0
Helena	MT	8.6	3.4	Tampa	FL	0	0
Hilo	HI	-	-	Toledo	OH	8.6	2.9
Honolulu	HI	-	-	Tonopah	NV	1.9	1.1
Houghton	MI	20.3	3	Topeka	KS	5	2.4
Houston	TX	0	0.1	Traverse City	MI	15.4	3.1
Huntington	WV	3.9	2.1	Tucson	AZ	0.1	0.1
Huntsville	AL	0.5	0.6	Tucumcari	NM	-	-
Huron	SD	12.3	4.2	Tulsa	OK	1.8	1.4
Indianapolis	IN	6	2.9	Victoria	TX	0	0.1
International Falls	MN	22.4	5.1	Waco	TX	0.2	0.2
Jackson	MS	0.2	0.3	Waterloo	IA	11.4	4.2
Jacksonville	FL	0	0.1	West Palm Beach	FL	0	0
Kahului	HI	-	-	Wichita Falls	TX	1	0.9
Kalispell	MT	-	-	Wichita	KS	3.6	2.1
Kansas City	MO	5.3	2.6	Wilkes-barre	PA	8.3	2.8
Key West	FL	-	-	Williamsport	PA	6.9	2.5
King Salmon	AK	-	-	Wilmington	DE	3.5	2.2
Knoxville	TN	1.5	1.1	Wilmington	NC	0.3	0.4
Kodiak	AK	-	-	Winnemucca	NV	3.7	2.5
Kotzebue	AK	-	-	Worchester	MA	11.6	4.1
La Crosse	WI	-	-	Yakima	WA	2.6	1.5
Lake Charles	LA	0	0.1	Yakutat	AK	-	-
				Youngstown	OH	9.8	2.6